Effect of Thermal Gradients Created by Electromagnetic Fields on Cell-Membrane Electroporation Probed by Molecular-Dynamics Simulations

J. Song,[1] A. L. Garner,[2] and R. P. Joshi[3,*]

[1]*Department of Electrical Engineering and Technology, Wentworth Institute of Technology, Boston, Massachusetts 02115, USA*

[2]*School of Nuclear Engineering, 400 Central Drive. Purdue University, West Lafayette, Indiana 47907-2017, USA*

[3]*Department of Electrical and Computer Engineering, Texas Tech University, Lubbock, Texas 79409, USA*

(Received 15 August 2016; revised manuscript received 16 December 2016; published 6 February 2017)

The use of nanosecond-duration-pulsed voltages with high-intensity electric fields (∼100 kV/cm) is a promising development with many biomedical applications. Electroporation occurs in this regime, and has been attributed to the high fields. However, here we focus on temperature gradients. Our numerical simulations based on molecular dynamics predict the formation of nanopores and water nanowires, but only in the presence of a temperature gradient. Our results suggest a far greater role of temperature gradients in enhancing biophysical responses, including possible neural stimulation by infrared lasers.

DOI: 10.1103/PhysRevApplied.7.024003

I. INTRODUCTION

The effects of pulsed electric fields on biological cells and tissues have been the topic of research since the late 1950s. In most applications, the electric pulses have been used as tools to modify various properties and responses of cells such as increases in membrane permeability for introducing various molecules and drugs into cells [1–5], fusion of cells [6,7], achieving physical separation [8], the killing of nonhealthy cells, and neuromuscular manipulation for therapy [9]. Interest in this area continues in numerous subareas of biomedical engineering [2,10–18]. More recently, high-intensity (∼100 kV/cm), nanosecond-duration-pulsed electric fields have been shown to be useful tools for cellular electroporation [19], electrically triggered intracellular calcium release [20,21], shrinkage of tumors [22,23], temporary blockage of action potential in nerves [24], and activation of platelets for accelerated wound healing [25]. Conceptually, short-duration pulses offer the possibility of triggering purely electrically driven responses without much thermal heating. In principle, then, fast processes such as electron transfers between molecules [26], electrophoretic separation and self-organization [27], or field-induced changes in reaction kinetics [28] could be fashioned, though detailed analyses and a complete understanding remain.

Most of the literature on the application of high-intensity ultrashort cellular pulses, except for a few reports [29–32], has ignored possible thermal effects because of the small (nanosecond) duration of the applied voltage pulses. One potential effect of local temperature enhancements is the increased fluidity of fatty-acid tails within the phospholipid bilayer which would facilitate membrane poration [29]. Here, we argue that issues associated with local heating should not be entirely dismissed. The importance of locally driven phenomena (such as sectional heating) cannot be overstated, even if globally averaged changes over the entire cell may remain negligible. As an example, localized calcium release (termed blips from single channels or puffs from a small collection of channels) can lead to global cellular signaling through a regenerative feedback mechanism [33]. More importantly, even if the temperature changes remained small and well controlled (to avoid nonlocal collateral damage), it is entirely conceivable that substantial local temperature gradients could be created. This issue of differential power dissipation in biological cells, which leads to temperature gradients, was first treated and discussed by Kotnik and Miklavčič [34]. It was shown that power dissipation within the membrane becomes much more pronounced in the MHz and lower GHz regions. In theory, a temperature differential across the outer cell membrane could be maintained by having an electromagnetic pulse train of relatively short duration (∼5 ns), as recently reported by Croce *et al.* [31]. They demonstrated that temperature differentials across the outer cell membrane in the 5–10-K range were entirely possible. For example, it was shown based on an equivalent lumped-circuit continuum analysis, that ultrashort high-intensity pulses could produce fast localized heating at the cell membrane, with the cytoplasm temperature being essentially unaffected [31]. Physically, this consequence arises from large differences between the conductivity of cell membranes and the cytosol. Croce *et al.* [31] predicted peaks of membrane temperature between 1 and 5 °C for single 10- and 1-ns pulses, respectively. For a typical 5-nm

*Corresponding author.
ravi.joshi@ttu.edu

cell membrane, Croce *et al.* [31] predicted membrane temperature gradients ranging from 0.2×10^9 to 10^9 K/m. Such possibilities of setting up thermal gradients also arise in the context of pulsed laser irradiation of cells [35], and radio-frequency or alternating current electric excitations [36]. Other specific ways to create temperature gradients include the use of nanoparticles in the vicinity of tumor cells, and subjecting the system to electromagnetic radiation [37,38], with thermal gradients as large as 10^8 K/m being reported a few years ago [39]. With laser excitation, temperature gradients of the order of 10^6 K m^{-1} can routinely be obtained in experiments [40].

The thermoelectric effect is a potentially relevant phenomenon associated with thermal gradients, and involves the development of an electric field. More recently, Bresme *et al.* [41] used molecular-dynamic (MD) simulations in water to show that a thermal gradient of 10^{10} K/m can result in the creation of an internal electric field of about 10^8 V/m. It was demonstrated that a thermal gradient polarizes water in the direction of the gradient, leading to a non-negligible electrostatic field whose origin lies in the water reorientation under nonequilibrium conditions. More specifically, the hydrogen atoms (or more generally the smaller of the two species in a polar molecule) begin pointing preferentially towards the cold region. Based on simple continuum mechanics, the electrostatic field (E) and the driving temperature gradient (dT/dr) are related as $E\sim(1-1/\varepsilon_r)(dT/dr)/T$, where ε_r is the dielectric constant. Hence, the electric field induced by the temperature gradient should be larger for high dielectric constant materials such as water. It is, therefore, very plausible that the creation of such fields driven by temperature gradients could enhance electroporation in biological cells. This aspect, however, has not been probed to the best of our knowledge. A more subtle point concerns the lifetime of the temperature gradient, and this can be understood from the following argument. When a thermal gradient is applied, the homogeneous system evolves to reduce the entropy production, which is made possible by creating an internal polarization. The heat transfer, which is dominated by intermolecular interactions and molecular polarization, is then reduced [42]. Thus, the polarized system as a whole becomes a less-effective heat conductor, implying that any local temperature increases and spatial gradients created would likely be sustained for a longer duration.

In any case, here we focus on thermal gradients as drivers for electroporative enhancements, even though the actual temperature values might not have changed appreciably from their equilibrium levels. Thus, aspects such as phase changes or protein denaturization are ignored, assuming that the absolute temperature changes due to such ultrashort pulses are minimal, around 1–5 °C at most [43]. Such a study is particularly relevant to high-intensity, nanosecond pulses which are inherently nonthermal in nature, but could establish large thermal gradients.

II. MODELING DETAILS

The dynamics of pore formation and water entry into a lipid bilayer membrane in response to an externally applied static-electric field is studied on the basis of MD simulations using the GROMACS package [44] with a 2-fs time step. Different temperatures are assigned to various regions to simulate the appropriate temperature gradients. The lipid membrane is taken to comprise dipalmitoyl-phosphatidylcholine (DPPC) molecules. A simple-point-charge water model mimicks the aqueous environment surrounding the membrane. Velocities of water and membrane molecules are generated randomly at each simulation run according to a Maxwellian distribution. Typically, MD simulations in such situations are carried out by selecting a segment of the lipid bilayer membrane and constructing an initial geometric arrangement of all the atoms and their bonding angles. Regions of water are then defined on either side of the membrane to form the total simulation space. The force fields for membrane molecular motion are taken from the literature [45], though more-recent updates with better force fields have been discussed by Siu *et al.* [46]. Here the somewhat older parameters are taken for simplicity and convenience. Simulations are at a constant particle number and assigned temperatures over local regions using a Berendsen thermostat [47] with a time constant of 0.1 ps. Weak pressure coupling (compressibility 4.5×10^{-5} bar^{-1}, time constant 1 ps) is employed for the z dimension. Long-range electrostatic interactions are computed with a particle mesh Ewald method [48] with a cutoff of 1 nm, a grid width of 0.15 nm, and periodic boundary conditions. A 0.9/1.2-nm group-based twin cutoff scheme is employed for the Lennard-Jones interactions. The linear constraint solver (LINCS) algorithm outlined by Hess *et al.* [49] is used to constrain all the bond lengths within the lipids and on the water geometry. The particle-mesh Ewald (PME) scheme is applied for long-range electrostatic interactions.

As is well known, the MD technique for any given simulation scenario can yield results that depend on the initial values assigned, specifically, the molecular velocities. Here, for statistical significance, a total of six MD simulations are carried out with different starting molecular velocities for the various conditions simulated and discussed in the next section. The trends are generally consistent, and the results shown in the next section represent a typical simulation outcome.

III. SIMULATION RESULTS AND DISCUSSION

The MD simulations are designed to probe the role of temperature gradients across the DPPC membrane on electroporation and water entry into the lipid bilayer. A constant electric field is used for each simulation, while the top and bottom surfaces of the membrane are assigned two separate fixed values. The water-membrane system contains 6323 water molecules and 128 DPPC lipid molecules

in a 6.9 nm × 7.4 nm × 7.0 nm simulation box. This membrane system is charge neutral and represents a homogeneous section of a simple lipidic membrane system.

The molecular-dynamics results obtained are discussed next. A 7-ns snapshot for a DPPC membrane set at a uniform temperature of 295 K is shown in Fig. 1. The central portion represents the membrane, while the water molecules are seen at the top and bottom on the *trans* and *cis* faces. This fixed-temperature case serves as a benchmark test case. A fairly high electric field of 0.4 V/nm is applied for these simulations. This high field provides an accelerated test of the biophysical process of pore formation, since low electric fields would otherwise take inordinately long simulation times. As seen in the 7-ns snapshot of Fig. 1 (which represents a typical outcome from a total of six simulation runs starting with different initial velocities), no pore is predicted to form in the membrane. A very slight protrusion at the bottom of the membrane near the middle represents a small and insignificant excursion of the water molecules, but with no beginnings of real pore formation.

To check whether any differences in the outcome may arise due to a temperature gradient, the MD simulations are performed once again on the same geometry, but with the top and bottom membrane surfaces kept at temperatures of 300 and 295 K, respectively. A snapshot from the MD simulations at 7 ns showing the molecular structure of the DPPC and water system is given in Fig. 2. A nanopore is clearly seen and a "water wire" is seen to connect the water reservoirs at the top and bottom. The entry of water molecules is slightly stronger at the top, which is the positive (anode) side and suggests a polarity dependence. This aspect was previously discussed by our group [16]. It is associated with the molecular stacking of the water network fashioned by the strong external electric field. Basically, in the case of freely rotating molecules, there is competition between energy reduction and the loss of orientational entropy upon alignment which is described by the well-known Langevin equation. For liquid water, orientations of water molecules are also subject to angle restrictions associated with hydrogen bonding and a strong tendency to minimize the loss of hydrogen bonds at the interface [50,51]. The hydrogen bonding between water molecules favors near-parallel dipole orientations relative to the membrane surface upon electric-field application. Hence to optimize hydrogen bonding, angular distributions of water molecules relative to the pore walls would be biased against orientations in which the hydrogen atoms point toward the circular walls. This, then, means that the water would likely enter from the outside at the anode end and move more easily from the inner membrane at the opposite cathode side. The prediction of a faster observable poration from the anode side has indeed been reported experimentally [52].

The difference in pore formation with temperature is again underscored by the results presented in Figs. 3. These MD simulations are carried out at a slightly higher field of 0.45 V/nm and the two snapshots shown are obtained at the longer 10-ns instant. Results shown in Fig. 3(a) are obtained at a constant temperature of 295 K; while for the case shown in Fig. 3(b), the membrane temperatures at the

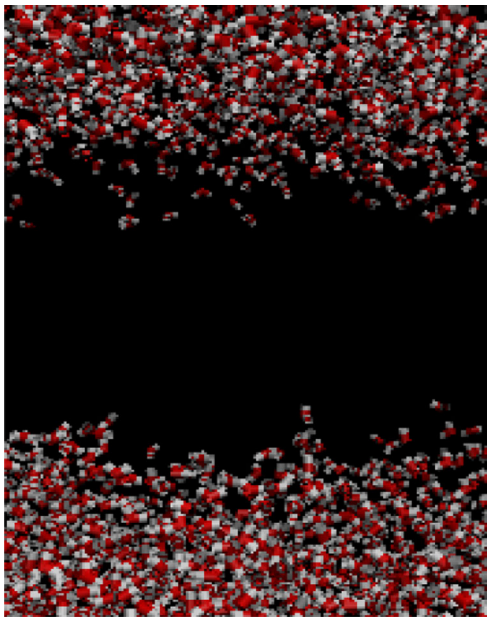

FIG. 1. A 7-ns snapshot of DPPC membrane section and adjoining water molecules subject to a constant 0.4-V/nm external electric field. A uniform temperature of 295 K is assumed.

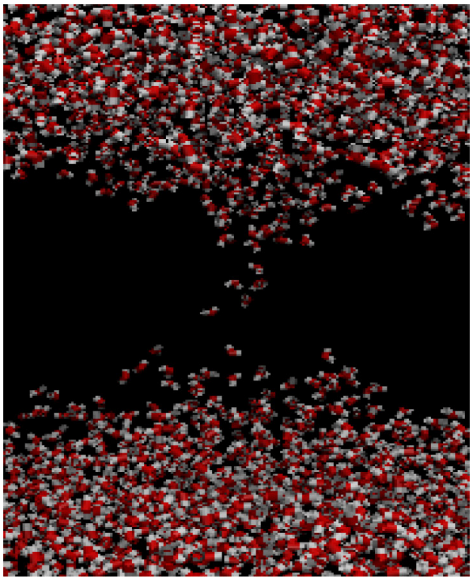

FIG. 2. A 7-ns snapshot of DPPC membrane section and the adjoining water molecules subject to a constant 0.4-V/nm external electric field. The membrane temperatures at the top and bottom are maintained at 300 and 295 K, respectively.

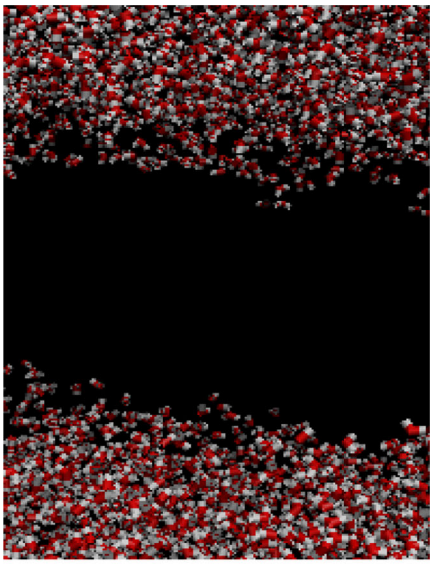

(a)

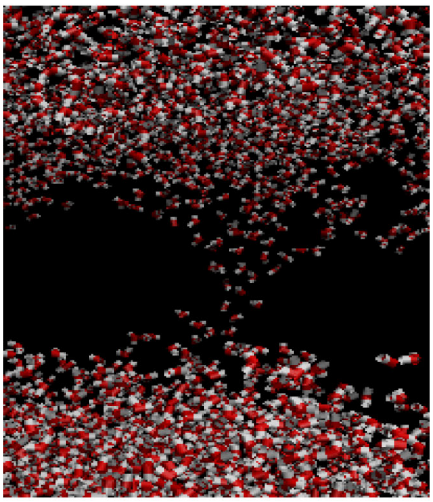

(b)

FIG. 3. A 10-ns snapshot of a DPPC membrane and the adjoining water molecules at a constant 0.45-V/nm external electric field. (a) Constant temperature of 295 K, and (b) different membrane temperatures at the top and bottom of 300 and 295 K, respectively.

top and bottom are chosen to be at 300 and 295 K, respectively. Despite the longer simulation time of 10 ns (as compared to 7 ns for Fig. 1) and the higher electric field, no pore formation is evident in Fig. 3(a). However, in Fig. 3(b), a nanopore is predicted. The initiation is once again from the upper anode end. Given the 5-nm membrane thickness, this result predicts that the 2×10^9 K/m temperature gradient would synergize electroporation.

The entire mechanism of electric-field creation due to internal thermal gradients in water perhaps requires a more detailed explanation and analysis, beyond just numerical MD simulations. This process is best understood in terms of system energy minimization. Assuming near-local equilibrium, the solvation energy G_{sol} (i.e., the single particle-free enthalpy) of a single sphere of diameter d is given by $G_{\mathrm{sol}} = -k_B T s d^2$, where k_B is the Boltzmann constant, T the absolute temperature, and s is a positive constant [53,54]. Incidentally, the solvation energy G_{sol} is related to the Soret coefficient S_T as $S_T = [1/(k_B T)]\, \delta G_{\mathrm{sol}}/\delta T$, which then leads to $S_T \sim -s d^2$. The linear dependence of the Soret coefficient (which is the ratio of the thermal diffusion coefficient to the ordinary diffusion coefficient) on the molecular area agrees with experimental results [55]. This Soret effect (also referred to as thermomigration, or the Ludwig-Soret effect), describes the mass flow induced by a temperature gradient in a fluid [56], and leads to the following equilibrium equation: $\nabla c + cST\, \Delta T = 0$, with "$c$" being the species concentration.

For the polar water molecules, one can crudely represent this as a dumbbell system having a dipole with two hard spheres of diameters "d_1" and "d_2". Considering such water molecules in a system having a spatial temperature gradient, the overall solvation energy for the molecular system would then be given as $G_{\mathrm{sol}} = -k_B s[T_1 d_1^2 + T_2 {d_2}^2]$, where $T_{1,2}$ are the local temperatures at the two spheres 1,2. Physically, the length scale of temperature variation is much larger than the length of the molecular dumbbell. Mathematically, these temperatures can be expressed in terms of the mean temperature at the midpoint as $T_{1,2} = T + (L/2)\{(T_1 - T_2)/L\} \equiv T \pm \Delta$, where $L \sim d_1 + d_2$ is the length of the dumbbell, and $T \sim (T_1 + T_2)/2$ is the average temperature in the vicinity of the water molecule. Denoting d_1 to be the diameter of the larger oxygen molecule, and the ratio of the diameters $d_1/d_2 = R$ (i.e., $R > 1$), one gets $G_{\mathrm{sol}} = -k_B s {d_2}^2[T(R^2+1) + \Delta(R^2-1)]$. Clearly, for minimizing the energy G_{sol}, one requires $\Delta > 0$. Hence, the temperature T_1 of the molecular system on the side containing the larger oxygen atom would be larger. More generally, the smaller of the two species systems in the polar molecule would begin pointing preferentially towards the colder region, in the presence of temperature gradients. It may also be pointed out that the effect would be stronger for polar molecules having a larger dipole separation distance L.

In addition to the separation L, the temperature can also be expected to play a role. More generally, the dipoles could be oriented at an angle θ with respect to the applied field direction. In this case, then, the average term $\langle \cos(\theta) \rangle = \int_0^\pi \cos(\theta) \sin(\theta) \exp[-G_{\mathrm{sol}}/(k_B T)] d\theta \} / 0 \int_0^\pi \sin(\theta) \exp[-G_{\mathrm{sol}}/(k_B T)] d\theta \}$ would have to be considered. In such a case, lower temperatures would provide a greater likelihood of orientation with the electric field. Also, at higher electric-field values, the dipoles could be better aligned and even form a possible lattice structure to enhance the Soret effect. Furthermore, if the outer membrane of a biological cell were subject to electric-field pulsing (with or without any additional optical or rf excitation), the outer side would be the hottest. For the

cell region facing the anode (e.g., the anodic polar cap), the electronegative oxygen atom of the polar water system would, consequently, be near the outer membrane, while the hydrogen would be a bit further away. This local polarized field would enhance the total field near the anode pole, and drive cellular electroporation more strongly. This is, thus, the essence of the additive synergy between a thermal gradient and an applied electric field.

The thermally induced polarization and development of an associated local electric field can, therefore, be seen to be a secondary and synergistic effect, while the primary driver for electroporation is the applied voltage. In fact, it is the electric fields in this case that would cause cellular heating, which would then lead to a differential thermal gradient. The thermal gradient would aid and assist in the electroporation process. In principle, poration at lower electric fields could occur, provided a significantly higher temperature difference is present to drive the process and achieve a comparable result. However, practically, there would be two issues with this route: (a) Elevating and then maintaining high temperature gradients would be difficult, and (b) phase transitions could easily occur at the higher temperatures or thermally activated detrimental cellular effects might be initiated. As a simple example, though, simulations at a lower 0.35-V/nm field are carried out with a 15-K thermal gradient, with the outer membrane kept at 310 K. A small "water wire" can be seen forming in Fig. 4, which is a 6.5-ns snapshot. Two different aspects are made obvious from this result. First, it is possible to electroporate at lower electric fields if higher temperature gradients are used. However, differential values of only up to 10 K have been reported [30], and so maintaining high temperature differentials across membranes would not be easy or practical. Second, the phase-transition temperature of DPPC is about 314 K [57], and so this sets another limit on the differential temperature. Though other much lower electric fields (for example, 0.25 V/nm) are tried for the MD simulations with at most a 313-K temperature for the outer membrane surface (i.e., a 18-K thermal differential), no nanopore formation is observed despite running the simulations up to 15 ns.

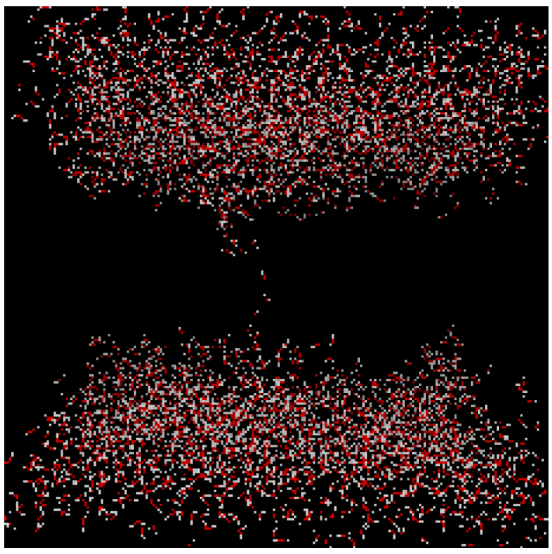

FIG. 4. A 6.5-ns snapshot of a DPPC membrane and the adjoining water molecules at a constant 0.35-V/nm external electric field. Different membrane temperatures at the top and bottom of 310 and 295 K, respectively, are used.

In any event, the development of an electrical field due to temperature gradients opens up possibilities for triggering various biophysical processes for a variety of applications. Here, the role of temperature gradients in facilitating electroporation has been probed. However, other forms of excitation (such as the use of infrared lasers) could also be used to create thermal gradients based on selective and spatially dependent absorption. The photothermal route would have the advantage over electrical stimulation in providing contact-free, spatially selective, artifact-free stimuli with both intensity- and wavelength-dependent variability. In fact, *in vivo* neural activation using low-intensity, pulsed infrared light for action potential generation at selected wavelengths has been reported recently in the literature [58,59]. The transient tissue temperature gradient is the likely driving mechanism based on measurements at the axon level; though the creation of membrane micropores (as studied in the present contribution) has also been proposed [60] as a possible alternate route. Other reports on infrared-induced neural activation suggest spatiotemporal temperature gradients to be an important causal driver [61] as well.

IV. CONCLUSIONS

The use of nanosecond-duration-pulsed voltages with high-intensity electric fields (∼100 kV/cm) is a recent development. The uses include irreversible electroporation for killing abnormal cells, reversible poration for drug and gene delivery, neuromuscular manipulation, electrically triggered intracellular calcium release as a second messenger, the shrinkage of tumors, and platelet activation for wound healing, etc. Dipole rotation, alignment, dielectrophoretic forces, Maxwell stress at the membrane, and even dielectric breakdown [62] have been some of the electrically driven mechanisms that have been invoked. However, thermal aspects have scarcely been discussed in the high-intensity, low-pulse-duration context. Here we have focused on the temperature gradients, since it is quite likely that despite modest changes in the temperature, a fairly large thermal differential could be attained across membranes given their nanoscale dimensions.

Molecular-dynamics simulations are carried out to probe the effects of differential temperatures across a cell membrane. For the same applied electric field, the formation of nanopores and water nanowires is clearly demonstrated, but only in the presence of a temperature gradient. Nanopores

with temperature gradients are predicted to form at lower values of the applied electric fields. This is one of the first numerical experiments showing enhanced electroporative effects arising from thermal gradients. The temperature gradient, though, is a secondary driver, with the electric field being the primary cause for electroporation. Even with thermal gradients, the electric-field range of around 0.5 V/nm is roughly comparable to that of previous predictions [63]. However, the study suggests a far greater (and perhaps universal) role of temperature gradients in fashioning and synergistically enhancing biophysical responses. For example, the observations of neural stimulation and changes in the transmembrane potentials by infrared lasers may also well be fundamentally tied to the process of creating localized thermal gradients.

ACKNOWLEDGMENTS

The authors thank S. Xiao (ODU) for useful discussions.

[1] E. Neumann, M. Schaefer-Ridder, Y. Wang, and P. H. Hofschneider, Gene transfer into mouse lyoma cells by electroporation in high electric fields, EMBO J. **1**, 841 (1982).

[2] L. M. Mir, S. Orlowski, J. Belehradek Jr., J. Teissié, M. P. Rols, G. Serša, D. Miklavčič, R. Gilbert, and R. Heller, Biomedical applications of electric pulses with special emphasis on antitumor electrochemotherapy, Bioelectrochem. Bioenerg. **38**, 203 (1995).

[3] G. Sersa, M. Cemažar, and D. Miklavcic, Antitumor effectiveness of electrochemotherapy with cis-diamminedichloroplatinum(II) in mice, Cancer Res. **55**, 3450 (1995).

[4] Y. Mouneimne, P. F. Tosi, R. Barhoumi, and C. Nicolau, Electroinsertion of full length recombinant CD4 into red blood cell membrane, Biochim. Biophys. Acta **1027**, 53 (1990).

[5] S. Raffy and J. Teissié, Insertion of glycophorin A, a transmembraneous protein, in lipid bilayers can be mediated by electropermeabilization, Eur. J. Biochem. **230**, 722 (1995).

[6] U. Zimmermann, Electric field mediated fusion and related electrical phenomena, Biochim. Biophys. Acta **694**, 227 (1982).

[7] A. E. Sowers, in *Cell Fusion* (Plenum, New York, 1987).

[8] W. M. Arnold, Positioning and levitation media for the separation of biological cells, IEEE Trans. Ind. Appl. **37**, 1468 (2001).

[9] R. Y. Wang, Y. R. Yang, M. W. Tsai, W. Y. J. Wang, and R. C. Chan, Effects of functional electric stimulation on upper limb motor function and shoulder range of motion in hemiplegic patients, American Journal of Physical Medicine and Rehabilitation **81**, 283 (2002).

[10] E. Neumann, S. Kakorin, and K. Toensig, The effect of resting transmembrane voltage on cell electropermeabilization: A numerical analysis, Bioelectrochem. Bioenerg. **48**, 3 (1999).

[11] J. Teissie, N. Eynard, B. Gabriel, and M. P. Rols, Electropermeabilization of cell membranes, Adv. Drug Delivery Rev. **35**, 3 (1999).

[12] R. P. Joshi and K. H. Schoenbach, Bioelectric effects of intense, ultrashort electric pulses, Crit. Rev. Biomed. Eng. **38**, 255 (2010).

[13] J. C. Weaver and Y. A. Chizmadzhev, Theory of electroporation: A review, Bioelectrochem. Bioenerg. **41**, 135 (1996).

[14] B. Rubinsky, Irreversible electroporation in medicine, Technol. Cancer Res. Treat. **6**, 255 (2007).

[15] M. P. Rols and J. Teissie, Electropermeabilization of mammalian cells to macromolecules: Control by pulse duration, Biophys. J. **65**, 1415 (1998).

[16] Q. Hu, Z. Zhang, H. Qiu, M. G. Kong, and R. P. Joshi, Physics of nanoporation and water entry driven by a high-intensity, ultrashort electrical pulse in the presence of cellular hydrophobic interactions, Phys. Rev. E **87**, 032704 (2013).

[17] J. C. Weaver, Electroporation of cells and tissues, IEEE Trans. Plasma Sci. **28**, 24 (2000).

[18] A. Golber and M. L. Yarmush, Nonthermal irreversible electroporation: Fundamentals, applications, and challenges, IEEE Trans. Biomed. Eng. **60**, 707 (2013).

[19] K. H. Schoenbach, R. P. Joshi, J. Kolb, N. Chen, M. Stacey, P. Blackmore, E. S. Buescher, and S. J. Beebe, Ultrashort electrical pulses open a new gateway into biological cells, Proc. IEEE **92**, 1122 (2004).

[20] S. J. Beebe, P. F. Blackmore, J. White, R. P. Joshi, and K. H. Schoenbach, Nanosecond pulsed electric fields modulate cell function through intracellular signal transduction mechanisms, Physiol. Meas. **25**, 1077 (2004).

[21] P. T. Vernier, Y. Sun, L. Marcu, S. Salemi, C. M. Craft, and M. A. Gundersen, Calcium bursts induced by nanosecond electric pulses, Biochem. Biophys. Res. Commun. **310**, 286 (2003).

[22] R. Nuccitelli, U. Pliquett, X. Chen, W. Ford, R. J. Swanson, S. J. Beebe, J. F. Kolb, and K. H. Schoenbach, Nanosecond pulsed electric fields cause melanomas to self-destruct, Biochem. Biophys. Res. Commun. **343**, 351 (2006).

[23] R. Nuccitelli, R. Wood, M. Kreis, B. Athos, J. Huynh, K. Liu, P. Nuccitelli, and E. H. Epstein, First-in-human trial of nanoelectroablation therapy for basal cell carcinoma: Proof of method, Experimental dermatology **23**, 135 (2014).

[24] R. P. Joshi, A. Mishra, J. Song, A. P. Pakhomov, and K. H. Schoenbach, Simulation studies of ultrashort, high-intensity electric pulse induced action potential block in whole-animal nerves, IEEE Trans. Biomed. Eng. **55**, 1391 (2008).

[25] K. H. Schoenbach, B. Hargrave, R. P. Joshi, J. F. Kolb, R. Nuccitelli, C. Osgood, A. P. Pakhomov, M. Stacey, R. J. Swanson, J. White, S. Xiao, J. Zhang, S. J. Beebe, P. F. Blackmore, and E. S. Buescher, Bioelectric effects of intense nanosecond pulses, IEEE Trans. Dielectr. Electr. Insul. **14**, 1088 (2007).

[26] A. Kranich, H. K. Ly, P. Hildebrandt, and D. H. Murgida, Direct observation of the gating step in protein electron transfer: Electric-field-controlled protein dynamics, J. Am. Chem. Soc. **130**, 9844 (2008).

[27] J. T. Groves, S. G. Boxer, and H. M. McConnell, Electric field-induced reorganization of two-component supported

bilayer membranes, Proc. Natl. Acad. Sci. U.S.A. **94**, 13390 (1997).
[28] P. M. De Biase, D. A. Paggi, F. Doctorovich, P. Hildebrandt, D. A. Estrin, D. H. Murgida, and M. A. Marti, Molecular basis for the electric field modulation of cytochrome *c* structure and function, J. Am. Chem. Soc. **131**, 16248 (2009).
[29] J. Song, R. P. Joshi, and K. H. Schoenbach, Synergistic effects of local temperature enhancements on cellular responses in the context of high-intensity, ultrashort electric pulses, Med. Biol. Eng. Comput. **49**, 713 (2011).
[30] V. Pierro, A. De Vita, R. P. Croce, and I. M. Pinto, Synergistic effects of local temperature enhancements on cellular responses in the context of high-intensity, ultrashort electric pulses, IEEE Trans. Plasma Sci. **42**, 2236 (2014).
[31] R. P. Croce, A. De Vita, V. Pierro, and I. M. Pinto, A thermal model for pulsed EM field exposure effects in cells at nonthermal levels, IEEE Trans. Plasma Sci. **38**, 149 (2010).
[32] J. T. Camp, Y. Jing, J. Zhuang, S. J. Beebe, J. Song, R. P. Joshi, and K. H. Schoenbach, Cell death induced by subnanosecond pulsed electric fields at elevated temperatures, IEEE Trans. Plasma Sci. **40**, 2334 (2012).
[33] S. Swillens, G. Dupont, L. Combettes, and P. Champeil, From calcium blips to calcium puffs: Theoretical analysis of the requirements for interchannel communication, Proc. Natl. Acad. Sci. U.S.A. **96**, 13750 (1999).
[34] T. Kotnik and D. Miklavčič, Theoretical evaluation of the distributed power dissipation in biological cells exposed to electric fields, Bioelectromagnetics (N.Y.) **21**, 385 (2000).
[35] A. L. Garner, V. B. Neculaes, M. Deminsky, D. V. Dylov, C. Joo, E. R. Loghin, S. Yazdanfar, and K. R. Conway, Plasma membrane temperature gradients and multiple cell permeabilization induced by low peak power density femtosecond lasers, Biochem. Biophys. Rep. **5**, 168 (2016).
[36] A. L. Garner, M. Deminsky, V. B. Neculaes, V. Chashihin, A. Knizhnik, and B. Potapkin, Cell membrane thermal gradients induced by electromagnetic fields, J. Appl. Phys. **113**, 214701 (2013).
[37] W. Chen and J. Zhang, Using nanoparticles to enable simultaneous radiation and photodynamic therapies for cancer treatment, J. Nanosci. Nanotechnol. **6**, 1159 (2006).
[38] H. H. Richardson, Z. N. Hickmaan, A. O. Govorov, A. C. Thomas, W. Zhang, and M. Kordesch, Thermooptical properties of gold nanoparticles embedded in ice: Characterization of heat generation and melting, Nano Lett. **6**, 783 (2006).
[39] A. O. Govorov, W. Zhang, T. Skeini, H. Richardson, J. Lee, and N. A. Kotov, Gold nanoparticle ensembles as heaters and actuators: Melting and collective plasmon resonances, Nanoscale Res. Lett. **1**, 84 (2006).
[40] H. R. Jiang, H. Wada, N. Yoshinaga, and M. Sano, Manipulation of Colloids by a Nonequilibrium Depletion Force in a Temperature Gradient, Phys. Rev. Lett. **102**, 208301 (2009).
[41] F. Bresme, A. Lervik, D. Bedeaux, and S. Kjelstrup, Water Polarization under Thermal Gradients, Phys. Rev. Lett. **101**, 020602 (2008).
[42] J. Muscatello, J. Romer, J. Sala, and F. Bresme, Water under temperature gradients: Polarization effects and microscopic mechanisms of heat transfer, Phys. Chem. Chem. Phys. **13**, 19970 (2011).
[43] A. G. Pakhomov, J. Doyle, B. E. Stuck, and M. R. Murphy, Effects of high power microwave pulses on synaptic transmission and long term potentiation in hippocampus, Bioelectromagnetics (N.Y.) **24**, 174 (2003).
[44] H. J. C. Berendsen, D. van der Spoel, and R. van Drunen, GROMACS: A message-passing parallel molecular-dynamics implementation, Comput. Phys. Commun. **91**, 43 (1995).
[45] W. F. van Gunsteren and H. J. C. Berendsen, *Gromos User Manual, BIOMOS Biomolecular Software* (Laboratory of Physical Chemistry, University of Groningen, Groningen, 1987).
[46] S. W. I. Siu, R. Vácha, P. Jungwirth, and R. A. Böckmann, Biomolecular simulations of membranes: Physical properties from different force fields, J. Chem. Phys. **128**, 125103 (2008).
[47] H. J. C. Berendsen, J. P. M. Postma, W. F. van Gunsteren, A. DiNola, and J. R. Haak, Molecular dynamics with coupling to an external bath, J. Chem. Phys. **81**, 3684 (1984).
[48] T. Darden, D. York, and L. Pedersen, Particle mesh Ewald: An $N \cdot \log(N)$ method for Ewald sums in large systems, J. Chem. Phys. **98**, 10089 (1993).
[49] B. Hess, H. Bekker, and H. J. Berendsen, LINCS: A linear constraint solver for molecular simulations, J. Comput. Chem. **18**, 1463 (1997).
[50] Q. Du, R. Superfine, E. Freysz, and Y. R. Shen, Vibrational Spectroscopy of Water at the Vapor/Water Interface, Phys. Rev. Lett. **70**, 2313 (1993).
[51] A. Luzar, S. Svetina, and B. Zeks, Consideration of the spontaneous polarization of water at the solid/liquid interface, J. Chem. Phys. **82**, 5146 (1985).
[52] P. T. Vernier, Y. Sun, L. Marcu, C. M. Craft, and M. A. Gundersen, Nanoelectropulse-induced phosphatidylserine translocation, Biophys. J. **86**, 4040 (2004).
[53] E. Eastman, Thermodynamics of non-isothermal systems, J. Am. Chem. Soc. **48**, 1482 (1926).
[54] E. Eastman, Theory of the Soret effect, J. Am. Chem. Soc. **50**, 283 (1928).
[55] S. Duhr and D. Braun, Thermophoretic Depletion Follows Boltzmann Distribution, Phys. Rev. Lett. **96**, 168301 (2006).
[56] S. Wiegand, Thermal diffusion in liquid mixtures and polymer solutions, J. Phys. Condens. Matter **16**, R357 (2004).
[57] Z. V. Leonenko, E. Finot, H. Ma, T. E. S. Dahms, and D. T. Cramb, Investigation of temperature-induced phase transitions in DOPC and DPPC phospholipid bilayers using temperature-controlled scanning force microscopy, Biophys. J. **86**, 3783 (2004).
[58] J. Wells, C. Kao, P. Konrad, T. Milner, J. Kim, A. Mahadevan-Jansen, and E. D. Jansen, Biophysical mechanisms of transient optical stimulation of peripheral nerve, Biophys. J. **93**, 2567 (2007).
[59] J. Wells, P. Konrad, C. Kao, E. D. Jansen, and A. Mashadevan-Jansen, Pulsed laser versus electrical energy for peripheral nerve stimulation, J. Neurosci. Methods **163**, 326 (2007).
[60] H. Hirase, V. Nikolenko, J. H. Goldberg, and R. Yuste, Multiphoton stimulation of neurons, J. Neurobiol. **51**, 237 (2002).
[61] M. G. Shapiro, K. Homma, S. Villarreal, C. P. Richter, and F. Bezanilla, Infrared light excites cells by changing their electrical capacitance, Nat. Commun. **3**, 736 (2012).
[62] U. Zimmermann, G. Pilwaat, and F. Riemann, Dielectric breakdown of cell membranes, Biophys. J. **14**, 881 (1974).